Plasmonically tunable blue shifted emission from Coumarin 153 in Ag nanostructure random media: A demonstration of fast dynamic surface enhanced fluorescence

Jayachandra Bingi, Vidya S, Anita R Warrier and C Vijayan*

Indian Institute of Technology Madras, Chennai-600036

*cvijayan@physics.iitm.ac.in

Abstract: Enhancement of intensity and wavelength tunability of emission are desirable features for light emitting device applications. We report on the large and tunable blue shift (60 nm) in emission from an environment-sensitive fluorophore (Coumarin153) embedded in Ag plasmonic random media. Coumarin 153 having emission at 555 nm, show a systematic blue shift (to 542 nm, 503 nm and 495 nm) upon infiltration into random media fabricated by Ag nanowires of different aspect ratio (hence surface plasmon resonances at 426 nm, 445 nm, 464 nm). The blue shift is due to fast dynamic surface enhanced fluorescence mechanism and can be tuned by controlling the surface plasmon resonance and hotspot density in random media. Enhanced emission at desired wavelength is achieved by using nanostructures having higher extinction coefficient but same surface plasmon resonance. Ag nanostructures of different aspect ratio used for fabricating the random media are synthesized by chemical route.

Key words: plasmonic random media, silver nanowires, blue shift, Coumarin153, extinction coefficient, radiative decay rate

1. **Introduction**

Plasmonic processes leading to enhancement and control of emission properties of fluorophore at close proximity of metal nanostructures is a topic of considerable recent interest in view of their applications in imaging, light emitting devices and sensors [1 - 3]. Most of the research work reported in this area focuses on metal-fluorophore interaction processes such as metal enhanced fluorescence (MEF) for emission intensity enhancement, surface plasmon coupled emission (SPCE) for directional and polarized emission and plasmon controlled fluorescence (PCF) of fluorophores in the proximity of metal nanostructures [4,5]. Plasmons squeeze incident electromagnetic (EM) fields within sub wavelength regions thus creating very high values of near field intensity around the metal nanostructure. The high near field intensities affect the electronic dynamics of fluorophore molecule, resulting in modifications in the decay rate and quantum yield [6]. Besides intensity enhancement (quantum yield), spectral modification also has been shown to be possible theoretically in plasmon induced emission studies [7].Only a few experimental reports are available on spectral modification of fluorophore molecules near plasmon nanostructures. M Ringler et al were able to shape the emission spectra of dye molecule by changing the distance between the particles in the nanoresonators by controlling the radiative and non radiative transition rates in the dye molecule [8]. Studies have also been done to modify the surface plasmon resonance by varying the surrounding environment [9, 10]. Tamitake Itoh et al demonstrated for the first time a clear blue shift in emission of rhodamine dyes in Ag dimer structures and Ag nanoclusters [11]. Spectral modification results from radiative and nonradiative decay rate modifications. An increase in the radiative decay rate results in blue shift in the emission spectrum of the fluorophore through a process known as fast dynamic surface enhanced fluorescence (FDSEF). However no reports are available on

achieving plasmon assisted blue shift in emission with intensity enhancement and tunability, which is particularly advantageous for light emitting device and sensing applications. This is equally significant in the study of sub-micron light-matter interactions such as FDSEF which is not exploited fully.

A random medium is an arrangement of particles or structures without spatial correlation. This provides an intense light-matter interaction through multiple scattering depending on size and dielectric properties of medium [12]. Hot spots (high spectral density regions) of the nanostructures are spread randomly throughout the plasmonic medium. It is reported that hotspot density enhances surface enhanced Raman scattering (SERS) [13, 14]. Assuming that hotspots are homogeneously distributed in random media, one can consider the higher near field effects on fluorophore emission that is infiltrated into it. Attaining FDSEF in plasmonic random media provides scope for tunable plasmonic random lasing applications.

Achieving FDSEF or blue shifted emission in plasmonic random media depends on several crucial aspects related to the choice of the fluorophore and medium. Since the surface enhanced fluorescence is due to coupling between excited dipole and local field, fluorophore molecules with higher excited state dipole moment are desirable. Further, the fluorophore must have high emission sensitivity to the surrounding environment in order to modify in emission spectra. The fluorophore chosen in the present work is Coumarin153 (C153) as its emission is sensitive to the polarity, viscosity and pH of the surrounding environment. Emission from C153 molecules is due to transitions occurring from ($\pi\pi^*$) excited states with larger dipole moments [15]. Plasmonic random media are prepared by Ag nanostructures with different aspect ratios. The choice of Ag is in view of the spectral matching between the plasmon resonance and the absorption peak of C153.

2. Experimental section

Ag nanowires are synthesised by a chemical method reported by Hu et al [16]. $AgNO_3$ (2 gm) and PVP (2.03 gm) are dissolved separately in 6 ml of Ethylene glycol (EG) and 34 ml of EG respectively. $AgNO_3$ solution is added drop wise to the PVP solution which is heated at 160 ^{0}C till the mixture turns white. This solution is kept at 160^{0}C for 40 min until it turns grey in colour. After allowing the solution to cool to room temperature, it is centrifuged and cleaned several times with ethanol for separating the Ag nano powder. Following the same procedure different samples are synthesized at pH values 2, 5, 7 and 9, these samples are labelled as S1, S2, S3 and S4 respectively.

Colloidal solutions of Ag nanostructures are prepared in ethanol with 1mM concentration. The random media are fabricated on glass substrates (2×1 cm^2) in the form of films by solvent evaporation technique. C153 laser dye (5 mM) in ethanol is infiltrated into these films by solvent evaporation technique. These dye-infiltrated samples prepared from samples S1, S2, S3 and S4 are labelled as CS1, CS2, CS3 and CS4 respectively. The label CS0 refers to the pure C153 coated over glass substrate.

The morphology is confirmed by QUANTA-400 Field Emission Scanning Electron Microscope (FESEM). Optical absorption measurements are done using JASCO V-570 spectrophotometer, and emission measurements are done using JASCO FP-6600 spectrofluorometer (for excitation at 400 nm) and HORIBA HR-800 UV laser Raman spectrometer (for excitation at 488 nm).

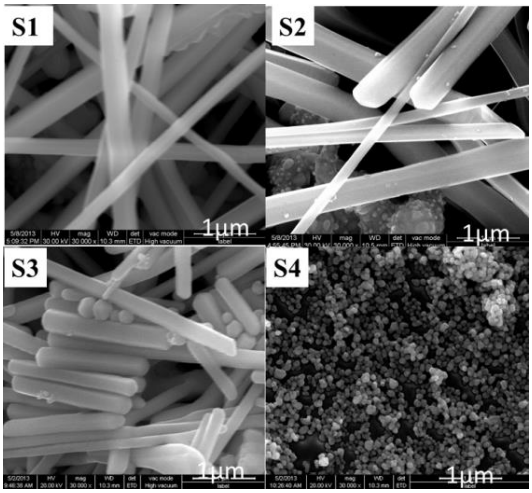

Figure 1: FESEM image of samples S1, S2, S3 and S4.

3. Results and Discussion:

FESEM images (figure 1) indicate that samples S1, S2 and S3 consist of nanowires of different aspect ratios. S1 and S2 are longer nanowires of mean diameters 252 nm and 510 nm with standard deviations 53 and 50 nm respectively whereas S3 is a shorter nanowire of mean diameter 299 nm with standard deviation 44 nm. Sample S4 consists of nanoparticles of mean diameter 92 nm with standard deviation 17 nm. The aspect ratio of samples is found to decrease (From S1 to S4) with increase in pH. The extinction spectra of these nanowires (S1, S2, and S3) dispersed in ethanol (1 mM solutions) is shown in Fig 2. The molar extinction coefficients calculated from the extinction spectra are 250, 290 and 630 $(M\ cm)^{-1}$ for S1, S2, and S3 respectively. The behaviour of the extinction coefficient is in accordance with the relation derived from Gans theory for metallic particles,

$$C_{ext} = I_m \left\{ \frac{\left(\varepsilon_{Ag} - \varepsilon_m\right)}{\left(\varepsilon_{Ag} + \chi\varepsilon_m\right)} \right\} \quad \text{..... (1)}$$

Where ε_{Ag}, ε_m and I_m are dielectric constants of silver and medium (air), and the incident intensity respectively, χ is the shape factor which increases with the increase in aspect ratio. Thus the equation quantifies the influence of the aspect ratio on the extinction coefficient. In

the present case the aspect ratio decreases from samples S1 to S3 [10]. Thus the sample S3 with a lower aspect ratio has a larger extinction coefficient.

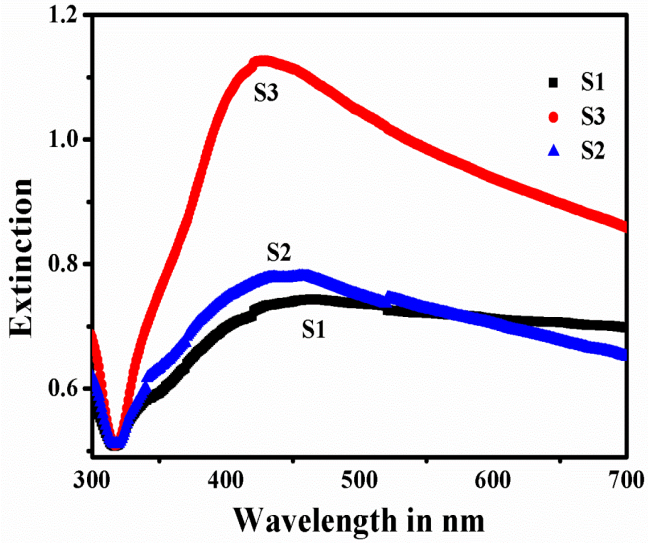

Figure 2: Extinction spectra of nanowire samples S1, S2 and S3.

The plasmonic resonance peaks of samples S1, S2 and S3 are at ~ 464 nm, 445 nm and 426 nm respectively. The variation in the plasmonic peak can be attributed to morphological variations like width and length of nanowires. It is observed that resonance shifts to shorter wavelengths (464 to 426 nm) as the aspect ratio decreases (from S1 to S3). The resonance peaks of sample S1 and S2 are broad compared to that of sample S3, which could be due to increased damping of plasmonic oscillations [17, 18]. However the processes of excitation as well as emission of the fluorophore can be influenced by the plasmonic peaks if they are sufficiently broad. Hence here the C153 fluorophore is chosen for infiltration into Ag random media, so that Ag surface plasmon resonance overlaps with both absorption and emission of C153.

Fig 3 shows the emission spectra for pure C153 film (CS0) and C153 infiltrated nanowires random media (CS1, CS2, and CS3), on excitation at 400 nm (3a) and 488 nm (3b). The excitation wavelengths are chosen to be on either side of the absorption peak of

pure C153 (~426 nm), so that emission can be observed at both excitations (400 nm, 488 nm) where the absorption cross sections are higher and lower respectively. Upon excitation at 400 nm, the pure C153 film (CS0) has its emission peak at ~ 555 nm. The emission peaks for the dye-infiltrated nanowire samples CS1, CS2 and CS3 occur at ~ 495 nm, 503 nm and 542 nm respectively. It clearly indicates effect of surrounding environment on C153 molecular emission, as CS1,CS2 and CS3 emit at different wavelengths. Fig. 3(b) shows the emission spectra for these samples on excitation at 488 nm. The blue shift shows a trend similar to that observed for excitation at 400 nm.

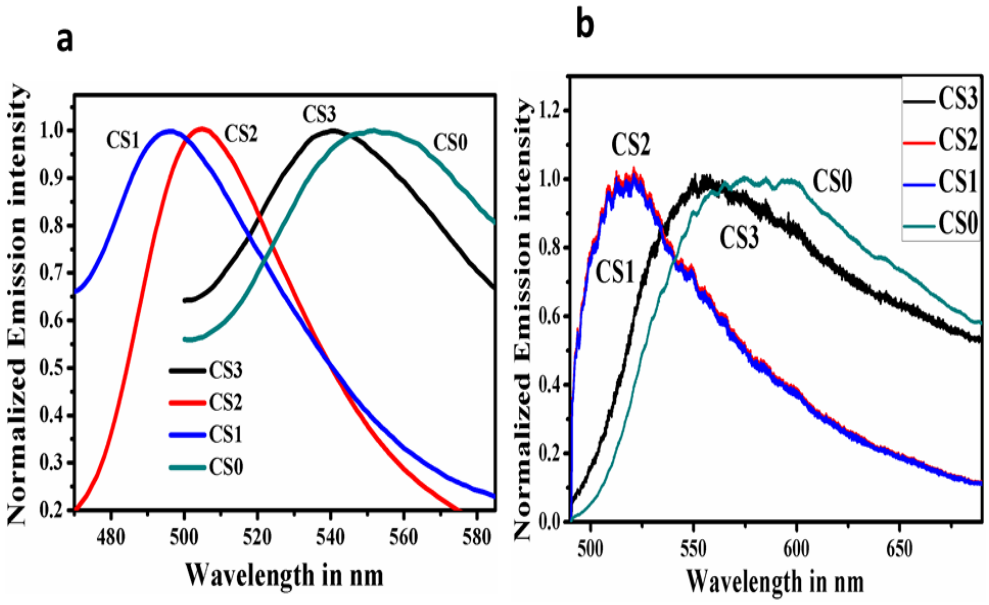

Figure 3:Emission spectra of pure C153 (CS0) and C153 infiltrated silver nanowires films (CS1, CS2, CS3) on excitation at (a) 400 nm and (b) 488nm.

For both excitations (400 nm and 488 nm), all samples show blue shift in emission in comparison to C153 free space emission. The fluorescence spectral modification also originates due to the formation of j-aggregates of fluorophore and charge transfer between fluorophore and metal structures [10, 19]. To confirm the origin of the blue shift, the extinction and emission spectra from two samples (CS2 and CS4), fabricated using S2 and S4 having same surface plasmon resonance (at 445 nm) but different morphology, is presented in

Fig. 4a and 4b. The blue shift obtained for both CS2 and CS4 is same with emission peaks at 503 nm. Thus the effect of plasmon resonance on spectral modification of C153 dye molecule is clearly demonstrated. The emission shift is independent of the morphology of the nanostructures and only depends on its plasmon resonances while the emission intensity is dependent on the morphology.

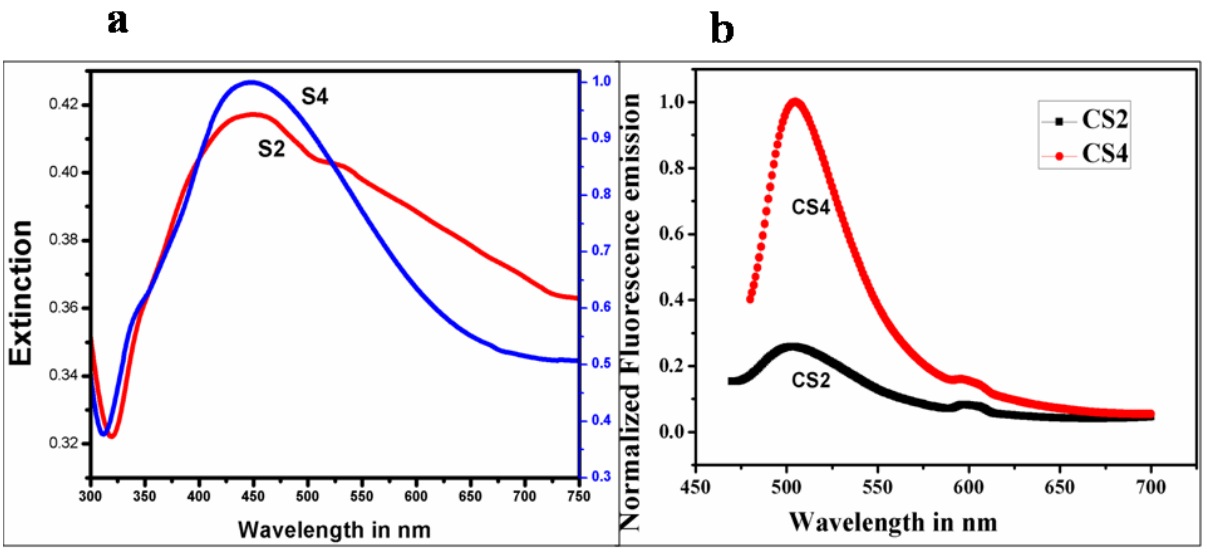

Figure 4: (a) Extinction spectra of S2 (nanowires) and S4 (nanoparticles) samples. (b) Emission spectra of C153 infiltrated S1 (nanowires) and S4 (nanoparticles) with excitation at 400 nm .

Observation of the emission spectra reveals several interesting features such as blue shift in emission, plasmon resonance dependent tunability and morphology dependent intensity enhancement. The blue shift can be explained in terms of the process fast dynamic surface enhanced fluorescence (FDSEF). As shown in figure 5, in free space, the internal relaxation rate (Γ_{int}) >>the total decay rate $\left(\Gamma_{rad}+\Gamma_{ET}+\Gamma_{nr0}\right)$, so radiative transitions occur from ω_0 to the ground state after several nonradiative transitions from ω_{ex} to ω_0. When the fluorophore molecule find itself in plasmonic environments (after infiltration into plasmonic random medium), depending on the field it experiences, the emission transition pathways are modified. In the presence of plasmonic field, the total decay rate becomes comparable to

internal relaxation rate ($\Gamma_{\text{int}} \le (\Gamma_{rad} + \Gamma_{ET} + \Gamma_{nr0})$), as a result the radiative transitions occur from vibrational states ω_{em} to ground states, leading to blue shift in the emission (Fig 5).

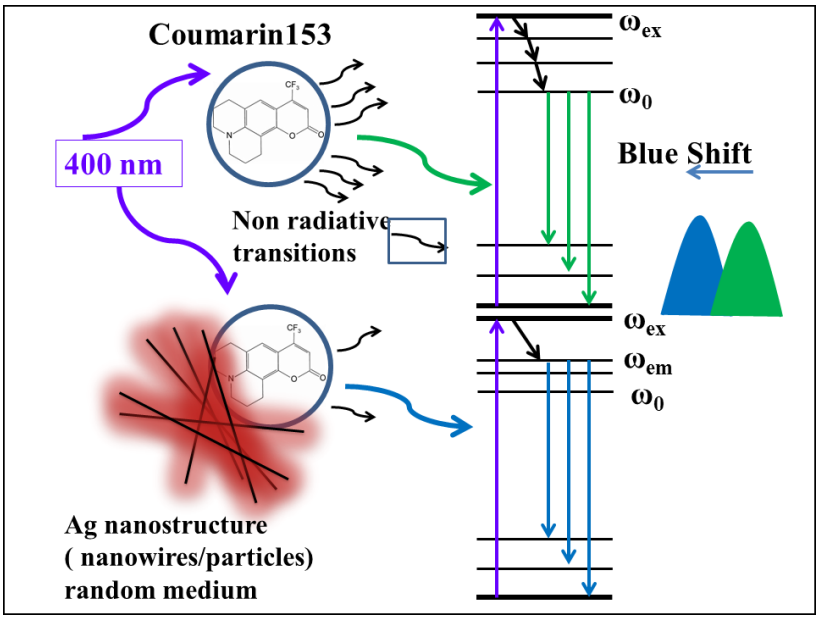

Figure 5: Illustration of electronic transitions in C153 in its pure form and when adsorbed on to the silver nanowire / particle random medium.

In FDSEF the density of emission states on the excitation λ_{ex} can be expressed as,

$$n_{FDSEF}(\omega_{em}) = \frac{\left| M_{ex}(\lambda_{ex}) \right|^2}{\eta_0(\omega_{em})} \left\{ \frac{\gamma_{r0}(\omega_{em} - \omega_{ex} + \omega_0) \left| M_{em}(\omega_{em}, d_{av}) \right|^2}{(\Gamma_{rad} + \Gamma_{ET} + \Gamma_{nr0})} \right\} \sigma_{abs}(\omega_{ex}) n_L(\omega_{ex}) \quad \text{.....} \quad (2)$$

where $M_{ex}(\lambda_{ex})$ is the enhancement occurring in excitation field at plasmonic nanostructure, $\eta_0(\omega_{em})$ is the quantum efficiency of fluorophore , $M_{em}(\omega_{em}, d_{av})$ is the enhancement in the emission field of fluorophore near the plasmon surface, $\gamma_{r0}(\omega_{em} - \omega_{ex} + \omega_0)$ is the radiative decay rate, Γ_{rad} is the total radiative decay rate, Γ_{ET} is the decay rate due to energy transfer from fluorophore excited dipole to plasmon, Γ_{nr0} is non radiative decay in ground state which

is independent of fields, $\sigma_{abs}(\omega_{ex})$ is the free space absorption crossection of the molecule at excitation ω_{ex} and $n_L(\omega_{ex})$ is excitation light power density [7,11].

Thus Eq-2, describes the dependence of density of emission states on the excitation power density ($n_L(\omega_{ex})$) and absorption crossection ($\sigma_{abs}(\omega_{ex})$) of C153 at excitation wavelength. Accordingly for all samples the emission spectra at 400 nm excitation is observable at lower excitation intensities, as the absorption crossection of C153 at 400 nm is comparatively high. But in the case of 488 nm excitation, where absorption crossection is less, emission is not observable for low excitation intensity. Hence a laser beam (Ar ion laser 488 nm) with 0.2 mW power is used for excitation to observe the emission.

Several features of FDSEF can be observed from emission spectra (Fig 3a, b), in the emission of CS3 (in both 3a and 3b) apart from the blue shifted emission (nm) it has notable emission at 555 nm, which is the free space emission of C153. This could be due to the slow dynamic surface enhanced fluorescence (SDSEF) which is the similar to FDSEF, gives only emission enhancement in the presence of high plasmon fields. Emission due to SDSEF is same as free space emission of fluorophore. FDSEF and SDSEF are generally coexisting. Emission of CS1 and CS2 samples has higher contribution from FDSEF than SDSEF, hence we find the blue shift is higher and emission at 555 nm is minimum. When the samples are excited with the 488 nm one can observe that emission of CS1 and CS2 abruptly come to zero near 488 nm which is another feature of FDSEF [11].

The emission tunability and its dependence on the surrounding plasmon environment of molecule are evident from the fig 3(a, b). This could be due to the increasing local field intensity experienced by fluorophore molecule in CS3 to CS1 that can alter the radiative and nonradiative transitions. Primarily the broad plasmon resonance peaks of CS1 and CS2 could be the reason for respective higher blue shifts because they can create of high

near fields and affect both emission and absorption levels of C153. Moreover the local field intensity inside the random media depends on the hot spot density which in turn depends on the surface roughness (sharp structures on the surface) and number of contact zones with other nanowires in the random media. In the case of CS1 and CS2 the blue shift is more where one can expect the large density of hotspots due to their higher lengths (aspect ratio) [20, 21]. Fig 6 shows the surfaces of the single nanowires in sample CS2 and CS3, it is clear that the sample CS2 which shows larger blue shift has sharper edges. In sample CS3 the hot spot density must be less as the length of individual nanowire is less, the surface is smooth and plasmon resonance curve is also comparatively narrower than CS1 and CS2. Thus all these facts lead to lower blue shift in emission of CS3. In addition to this the possibility of mode coupling and interference effects also contribute to the local field in random media [22, 23], making the process complicated for developing an exact relation between plasmon resonance and emission shift.

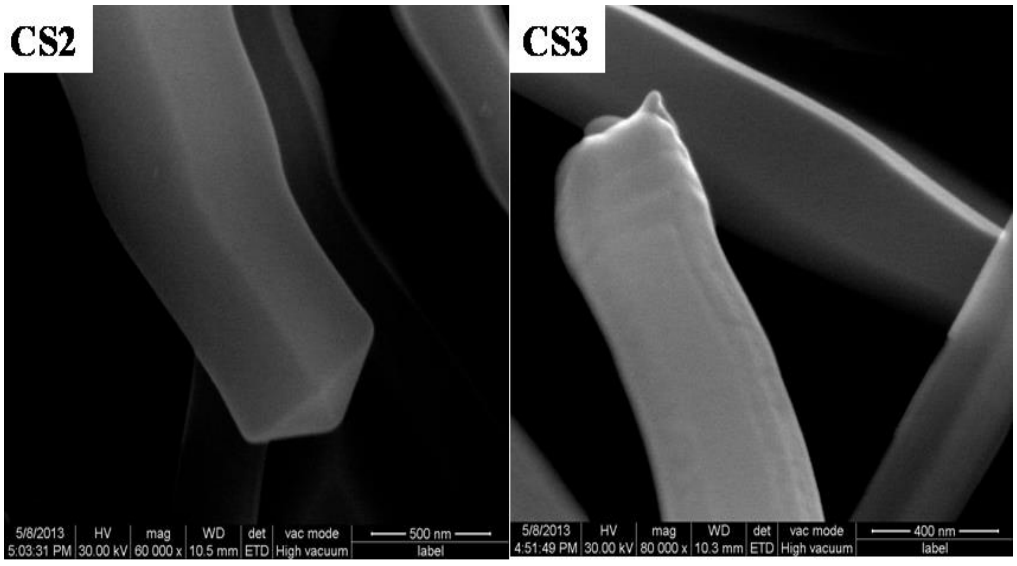

Figure 6: FESEM image of single nanowires of CS2 and CS3.

From Fig 4b, there is a clear enhancement in emission intensity of CS4 (nanoparticles random media) over CS2. This can be explained from Eq 2 where the emission field enhancement $M_{em}(\omega_{em}, d_{av})$ depends on the extinction rate of the nanostructure. The extinction is high for nanoparticles than nanowires shown in figure 4a. Thus by controlling the extinction of nanostructures with same plasmon resonance one can tune the intensity of emission at desired wavelength.

4. Conclusion:

Fast dynamic surface enhanced fluorescence is demonstrated in plasmonic random media fabricated from Ag nanostructures of different aspect ratios and varying plasmon resonances. Fluorophore (C153)-silver nanostructure random media are fabricated by solvent evaporation method and the emission from the fluorophore is found to be blue shifted with respect to its free space emission. The emission wavelength shows a blue shift from 555 nm to 495 nm with increase in the plasmon resonance wavelength (426 nm- 464 nm) of nanostructure with which the random media are fabricated. Enhancement of emission intensity is achieved by using random media having higher extinction coefficient.

Utilization of plasmonic random media to obtain tunable and enhanced fluorescence based on fast dynamic surface enhanced fluorescence is a rather new paradigm in the design of efficient light emitting devices and sensors. This is significant also from the point of view of achieving tunable random lasing at lower thresholds by the choice of an appropriate combination of a dye and a plasmonic nanostructure.

References

1. Tian M, Huanjun C, Ruibin J, Qian L and Jianfang W (2012) Plasmon-Controlled Fluorescence beyond the Intensity Enhancement. J. Phys. Chem. Lett., 3, 191−202.
2. Hobson PA, Wedge S,Wasey JAE, Sage I, Barnes WL(2002) Surface Plasmon Mediated Emission from Organic Light-Emitting Diodes. Adv. Mater. 14, 1393−1396.
3. Haes AJ, Haynes CL, McFarland AD, Schatz GC, Van DRP , Zou S L (2005**)** Plasmonic Materials for Surface-Enhanced Sensing and Spectroscopy**,**MRS Bull., 30, 368−375.
4. Ray. K , Chowdhury MH, Zhang J, Fu Y,Szmacinski H,Nowaczyk K,Lakowicz JR (2010)Plasmon-controlled fluorescence towards high-sensitivity optical sensing. Optical Sensor Systems in Biotechnology :Advances in Biochemical Engineering / Biotechnology. Springer publications.
5. Ying J, Hai-YW, Hai W, Bing-RG, Ya-wei H, Yu J, Qi-DC, Hong-BS (2011) Surface Plasmon Enhanced Fluorescence of Dye Molecules on Metal Grating Films. J. Phys. Chem. C, 115, 12636–12642.
6. Geddes CD and Joseph RL (2002) Metal-Enhanced Fluorescence Journal of Fluorescence, 12, No. 2, 121-129.
7. Le REC, Etchegoin PG, Grand J, Felidj N, Aubard J, Levi G.(2007) Mechanisms of Spectral Profile Modification in Surface-Enhanced Fluorescence. J. Phys. Chem. C. lett, 111, No. 44, 16076-16079.
8. Ringler M, Schwemer A, Wunderlich M, Nichtl A, Ku¨rzinger K, Klar TA, Feldmann J (2008) Shaping Emission Spectra of Fluorescent Molecules with Single Plasmonic Nanoresonators. Phys. Rev. Lett, 100, 203002.
9. Zhao L,Ming T,Chen H J, Liang Y, Wang JF (2011). Plasmon-Induced Modulation of the Emission Spectra of the Fluorescent Molecules near Gold Nanorods. Nanoscale 3, 3849−3859.
10. Jing Z, Lasse J, Jiha S, Shengli Z, George CS, Richard PVD (2007). Interaction of Plasmon and Molecular Resonances for Rhodamine 6G Adsorbed on Silver Nanoparticles, J.Am.Chem.Soc, 129, 7647-7656.
11. Tamitake I,Yuko SY,Hiroharu T,Vasudevanpillai B, Norio M, Yukihiro O (2013).Excitation laser energy dependence of surface-enhanced fluorescence showing plasmon-inducedultrafast electronic dynamics in dye molecules, Phys.Rev. B, 87, 235408.
12. Pedro DG, Riccardo S, Álvaro B, López C (2007) Photonic Glass: A Novel Random Material for Light, Adv. Mater., 19, 2597–2602.
13. Yongwen T,Jiajun G, Linhua X, Xining Z,Dingxin L, Wang Z, Qinglei L,Shenmin Z,Huilan S,Chuanliang F,Genlian F, Di Z (2012), High-Density Hotspots Engineered by Naturally Piled-Up Subwavelength Structures in Three-DimensionalCopper Butterfly Wing Scales for Surface-Enhanced RamanScattering Detection.Adv. Funct. Mater. 22, 1578–1585.
14. Daniel A. C, Tyler E. McPherson,Shanlin P,Mingyang C, David A, Dixonand DH (2013).Spatial and temporal variation of surface-enhanced Raman scattering at Ag nanowires in aqueoussolution.Phys.Chem. Chem. Phys, 15, 850.

15. Brian D. W (2009). The Use of Coumarins as Environmentally-Sensitive Fluorescent Probes of Heterogeneous Inclusion Systems. Molecules, 14, 210-237.
16. Mingjun H, Jiefeng G, Yucheng D, Shiliu Y, Robert KYL (2012). Rapid controllable high-concentration synthesis and mutual attachment of silver nanowires.RSC Advances, 2, 2055–2060.
17. Sönnichsen C,Franzl T,Wilk T, von PG,Feldmann J, Wilson O ,Mulvaney P (2002). Drastic Reduction of Plasmon Damping in Gold Nanorods.Phys. Rev. Lett, 88,no 7, 077402.
18. Kolwas K,Derkachova A (2013). Damping rates of surface plasmons for particles of size from nano- to micrometers reduction of the nonradiative decay. Journal of Quantitative Spectroscopy & Radiative Transfer, 114, 45-55.
19. John R. L, Ronald L B, Tianhong L, Jia X, (1986) Charge-transfer theory of surface enhanced Raman spectroscopy: Herzberg–Teller contributions, J. Chem. Phys. **84**, 4174.
20. Miaosi C, In Y P,Mian R L, Joel K W Y Xing Y L (2013).Layer-By-Layer Assembly of Ag Nanowires into 3D Woodpile-like Structures to Achieve High Density "Hot Spots" for Surface-Enhanced Raman Scattering.Langmuir, 29, 7061−7069.
21. Benjamin M, Ross , Luke P L (2009).Creating high density nanoantenna arrays via plasmon enhanced particle–cavity (PEP–C) architectures.Opt. Express. 17, 8, 6860.
22. Martina A, Yudong W, Pablo A, de GCH., Javier A, Muskens O (2012). Interference, Coupling, and Nonlinear Control of High-Order Modes in Single Asymmetric Nanoantennas.ACS NANO, 6, NO. 7, 6462–6470.
23. Novotny L, Hecht B , Pohl DW (1997). Interference of locally excited surface plasmons. J. Appl. Phys. 81 (4), 1798-1806.